



“Flow-void” sign in osseous metastatic renal cell carcinoma

J. Murphy*, A. Patel, S.L. James, R. Botchu, A.M. Davies

Royal Orthopaedic Hospital, Bristol Road South, Birmingham B31 2AP, UK

ARTICLE INFORMATION

Article history:

Received 2 May 2018

Accepted 9 August 2018

AIM: To evaluate the frequency of the “flow-void” sign in a large series of pathologically proven renal cell carcinoma (RCC) bone metastases referred to a specialist unit and to evaluate its correlation with both lesion size and imaging sequence. A further aim was to describe a proposed grading system for the description of the “flow-void” sign.

MATERIALS AND METHODS: A retrospective review of patients with magnetic resonance imaging (MRI) of pathologically proven RCC bone metastases between September 2007 and December 2017 was performed. MRI images were reviewed for the presence of the “flow-void” sign and a proposed grading system for this sign was applied. Statistical analysis was performed to determine the association between the presence of the “flow-void” sign and lesion size and MRI sequence.

RESULTS: One hundred and forty bone lesions in 123 patients with histologically proven metastatic RCC were reviewed. One hundred and thirty-two (94.3%) lesions demonstrated the “flow-void” sign on at least one sequence in each study. A statistically significant difference was demonstrated between lesion size and the presence and type of “flow-void” sign. Lesions demonstrating type 3 “flow-void” sign had mean dimensions of 82.2 mm compared to 47.3 mm for lesions that did not demonstrate the “flow-void” sign ($\chi^2(2) = 11.4$; $p = 0.01$). T2-weighted, proton density and fat-saturated imaging also demonstrated the “flow-void” sign more frequently.

CONCLUSION: The “flow-void” sign is a common imaging feature within RCC bone metastases. When observed, the “flow-void” sign can be a useful imaging feature in the diagnosis of RCC bone metastases.

© 2018 The Royal College of Radiologists. Published by Elsevier Ltd. All rights reserved.

Introduction

Renal cell carcinoma (RCC) accounts for approximately 5% of adult cases of cancer in men and 3% in women.¹ It is known for its strong metastatic potential. Metastatic disease is diagnosed at presentation in up to 18% of patients with RCC¹ and during follow-up, post-nephrectomy in 50%

of patients.² Bone is the second most common site of metastasis in metastatic RCC and is involved in 20–60% of patients.^{3–6}

A bone metastasis from a clinically occult primary tumour is frequently the mode of presentation in patients with RCC,^{7–9} as seen in 48% of patients with RCC bone metastases.¹⁰ Solitary bone metastases are relatively frequent in patients with RCC. They have been reported to occur in up to 2.5% of all patients with RCC,^{3,11} with bone being the most common site. Imaging features of many bone tumours are non-specific. A RCC bone metastasis, particularly if solitary, can mimic a malignant primary bone

* Guarantor and correspondent: J. Murphy, Royal Orthopaedic Hospital, Bristol Road South, Birmingham B31 2AP, UK. Tel.: +44 (0) 121 685 4135; fax: +44 (0) 121 685 4108.

E-mail address: jennifer.murphy7@nhs.net (J. Murphy).

tumour, and its diagnosis on imaging often relies on the availability of adequate clinical information.

The “flow-void” sign is a distinctive imaging feature in RCC initially described by Choi *et al.*¹² in 2003; however, little attention has been paid to this sign since then, with just one PubMed citation and 24 Google Scholar citations, eight of which related to RCC bone metastases. Flow voids result from signal loss due to blood flowing out of the section before the signal can be sampled, and are therefore, a manifestation of rapid flow in arteries and also turbulence-related dephasing.¹³ They are demonstrated as serpiginous, tubular areas without signal on all pulse sequences and correlate well with the presence of pathological vessels.^{1,12} Flow voids have also been described in other bone lesions, including benign lesions, such as haemangiomas, and in rare vascular tumours, such as angiosarcoma and haemangiopericytoma.

The purpose of the present study was to evaluate the frequency of the “flow-void” sign in a large series of pathologically proven RCC bone metastases referred to a specialist unit and to evaluate the correlation between the “flow-void” sign and both lesion size and imaging sequence. From the authors’ experience, the morphology of the “flow-void” sign can vary. Therefore, a further aim was to describe a proposed grading system for the description of the “flow-void” sign.

Materials and methods

Patients

A retrospective search was performed using the radiology information system to identify patients with RCC bone metastases. Patients with magnetic resonance imaging (MRI) performed between September 2007 and December 2017 were included in the study. Patient demographics, the site and dimensions of bone lesions, and the presence of single or multiple lesions were recorded. The history of known RCC prior to presentation with the index bone lesion was also recorded using the oncology database. The study was registered with the institutional review board. Ethical approval was not required for the retrospective review of imaging used in this study.

Imaging

MRI imaging was performed using a 3 T MRI system (Magnetom Skyra; Siemens, Erlangen, Germany). MRI images were obtained in at least three orthogonal planes in each patient with a section thickness of 3–10 mm. Intravenous gadolinium was not routinely administered. Patients with MRI performed in external institutions were also included in the study.

Image evaluation

MRI was reviewed by four consultant musculoskeletal radiologists and one fellow for the presence of the “flow-void” sign. The “flow-void” sign was defined as the presence

of multiple dot-like or tubular structures with low signal intensity located within or around the lesion. A grading system was applied retrospectively for the “flow-void” sign by one reader when present (Fig 1). Type 1 was defined as multiple punctate areas without signal on all pulse sequences within or surrounding the lesion. Type 2 was defined as serpiginous, tubular areas of signal void on all pulse sequences visible on fewer than three consecutive sections, measuring <3 mm in diameter. Type 3 was defined as multiple serpiginous, tubular areas of signal void on all pulse sequences visible on three or more consecutive sections, measuring ≥3 mm in diameter. Radiographs were also reviewed to evaluate for matrix mineralisation or trabeculation, which could simulate the “flow-void” sign.

Statistical analysis

Statistical analysis was performed with SPSS software (released 2016, version 24.0; IBM SPSS Statistics for Mac, Armonk, NY, USA). Descriptive statistics were calculated. The Kruskal–Wallis *H*-test was used to calculate the difference between lesion size and the presence and type of “flow-void” sign. The association between the presence and type of “flow-void” sign and type of MRI sequence was calculated using a Pearson chi-square test. A *p*-value of <0.05 was considered statistically significant.

Results

One hundred and forty bone lesions in 123 patients with histologically proven metastatic RCC were reviewed. Patient demographics are detailed in Table 1. The mean age in the patient cohort was 62.9 (range 36–84) years and 79 (64.2%) patients were male. In the present patient cohort, 50.4% presented with symptoms of bone metastases or pathological fracture without a known prior history of RCC. One hundred and four (84.6%) patients presented with a solitary lesion at diagnosis, while the remaining patients presented with two or more lesions.

Radiological findings are detailed in Table 2. In the present patient cohort, the mean size of RCC bone metastases at presentation was 67.4 mm, with a range of 16–63 mm. Ninety-nine (69.7%) lesions were present within long bones, 57.6% of which occurred in the proximal long bone. The pelvis was the next most common site (24 [16.9%] lesions). One hundred and thirty-two (94.3%) lesions demonstrated the “flow-void” sign on at least one sequence in each study. A statistically significant difference was demonstrated between lesion size and the presence and type of “flow-void” sign (Table 3). Lesions demonstrating type 3 “flow-void” sign had mean dimensions of 82.2 mm compared to 47.3 mm for lesions that did not demonstrate the “flow-void” sign.

Six-hundred and thirty-six sequences were reviewed in this patient cohort. MRI sequences performed are detailed in Table 4. Axial and coronal T1-weighted and coronal short-tau inversion recovery (STIR) sequences were performed most frequently. The association between the presence and type of “flow-void” sign and MRI sequence is

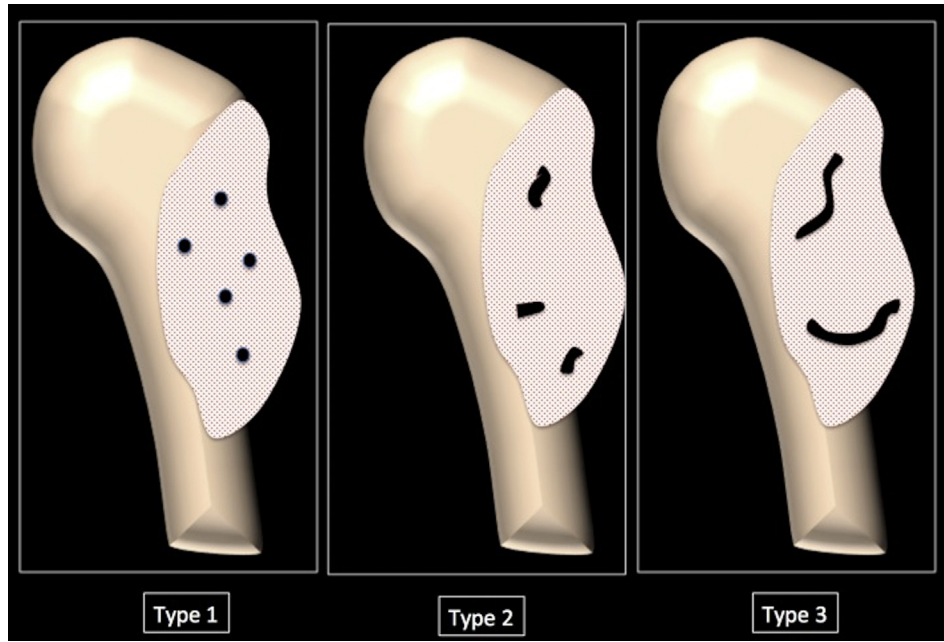


Figure 1 Grading system used for the evaluation of the “flow-void” sign on MRI.

detailed in Table 5. In the present cohort, a statistically significant association was found between the presence of the “flow-void” sign and both the type of sequence and the use of fat saturation ($\chi^2 = 23.0$; $p = 0.001$ and $\chi^2 = 30.6$; $p = 0.00$, respectively). The “flow-void” sign was more frequently demonstrated on T2-weighted and proton-density (PD) imaging rather than T1-weighted imaging (Figs 2–4). In addition, PD imaging demonstrated type 2 and type 3 “flow-void” sign most frequently (75.4% of PD sequences, Figs 3 and 4). The “flow-void” sign was also seen more frequently in fat-saturated compared to non-fat-saturated imaging (Fig 4). Type 2 and type 3 “flow-void” sign was demonstrated more frequently in fat-saturated imaging (70.6% of fat-saturated sequences). A statistically significant association was not found between the plane of imaging and presence of the “flow-void” sign ($\chi^2 = 4.7$; $p = 0.58$).

Discussion

Bone is the second most common site of metastasis from RCC and is associated with a poor prognosis. Shortened

Table 1
Patient demographics and clinical history.

Age	Mean 62.9 years (range 36–84)
Gender	n=123
Male	79 (64.2%)
Female	44 (35.8%)
Prior history of RCC	n=123
Known history of RCC	61 (49.6%)
No prior history	62 (50.4%)
No. of lesions at presentation	n=123
Single lesion	104 (84.6%)
≥2 lesions	19 (15.4%)

survival has been reported in patients with RCC bone metastases compared to other metastatic sites.^{14,15} Targeted treatment such as surgical resection, radiotherapy, and percutaneous transcatheter arterial embolisation have been shown to be safe and reliable for restoring mechanical bone stability, relieve pain, improve mobility, and provide good function in most patients with RCC bone metastases.^{5,10,16–22}

Similar to other bone tumours, imaging of RCC bone metastases can be non-specific. The “flow-void” sign in RCC bone metastases was initially described in 2003 by Choi et al.¹² In this small study of 16 patients, the “flow-void” sign was identified in up to 80% of lesions and correlated well with the presence of pathological vessels on computed tomography and digital subtraction angiography. A further study of 13 patients with RCC bone metastases published in 2009 also reported the presence of flow voids in 80% of

Table 2
Radiological findings.

Maximum dimension (mm)	Mean 67.4 mm (range 16–163)
Site of lesions	(n=140)
Long bones	99 (69.7%)
Proximal	57 (57.6%)
Diaphysis	20 (20.2%)
Distal	22 (22.2%)
Pelvis	24 (16.9%)
Scapula	5 (3.5%)
Vertebral column	8 (5.6%)
Clavicle	3 (2.1%)
Sternum	1 (0.7%)
Patella	1 (0.7%)
Phalanx	1 (0.7%)
“Flow-void” sign	(n=140)
Absent	8 (5.7%)
Present	132 (94.3%)

Table 3
Difference in lesion size between the presence and type of “flow-void” sign.

“Flow-void” sign	N	Mean dimension (mm)
Absent	8	47.3
Type 1	17	54
Type 2	53	65.6
Type 3	62	82.2

$\chi^2(2)=11.4; p=0.01$

Table 4
Magnetic resonance imaging (MRI) sequences performed (n=636).

Sequence	Axial	Coronal	Sagittal
T1	105 (16.5%)	109 (17.1%)	38 (6%)
T2	32 (5%)	6 (0.9%)	20 (3.1%)
Fat-saturated T1	3 (0.5%)	1 (0.2%)	0
Fat-saturated T2	67 (10.5%)	6 (0.9%)	6 (0.9%)
STIR	28 (4.4%)	93 (14.6%)	28 (4.4%)
T1 post-gadolinium	6 (0.9%)	4 (0.6%)	2 (0.3%)
Fat-saturated T1 post-gadolinium	10 (1.6%)	6 (0.9%)	5 (0.8%)
PD	9 (1.5%)	1 (0.2%)	5 (0.8%)
Fat saturated PD	16 (2.5%)	16 (2.5%)	14 (2.2%)

STIR, short tau inversion recovery; PD, proton density.

Table 5
Association between magnetic resonance imaging (MRI) sequences and presence and type of “flow-void” sign (n=636).

“Flow-void” sign	T1-weighted	T2-weighted	Proton-density weighted
Absent	71 (24.6%)	37 (12.9%)	6 (9.8%)
Type 1	45 (15.6%)	60 (21%)	9 (14.8%)
Type 2	101 (34.9%)	95 (33.2%)	30 (49.2%)
Type 3	72 (24.9%)	94 (32.9%)	16 (26.2%)

$\chi^2=23; p=0.001$

“Flow-void” sign	Fat saturated	Non-fat saturated
Absent	27 (9%)	87 (25.8%)
Type 1	61 (20.4%)	53 (15.7%)
Type 2	115 (38.5%)	111 (32.9%)
Type 3	96 (32.1%)	86 (25.5%)

$\chi^2=30.6; p=0.00$

“Flow-void” sign	Axial	Coronal	Sagittal
Absent	49 (17.8%)	46 (19%)	19 (16.1%)
Type 1	54 (19.6%)	36 (14.9%)	24 (20.3%)
Type 2	98 (35.5%)	92 (38%)	36 (30.5%)
Type 3	75 (27.2%)	68 (28.1%)	39 (33.1%)

$\chi^2=4.7; p=0.58$

lesions.²³ In the present cohort of 123 patients, the “flow-void” sign was present in 94.3% of RCC bone metastases. The “flow-void” sign is potentially a useful sign in general radiological practice. Although the specificity of the “flow-void” sign is unknown, its presence on MRI should raise the suspicion of RCC bone metastases. When the suspicion for RCC bone metastases is raised, further investigations can be initiated to evaluate for an occult primary renal tumour. Moreover, the “flow-void” sign should also serve as an indicator of hypervascularity when considering biopsy or other intervention of the lesion.

In the authors’ experience, the “flow-void” sign can be subjective and vary in morphology. Therefore, a grading system for the “flow-void” sign was also described. This

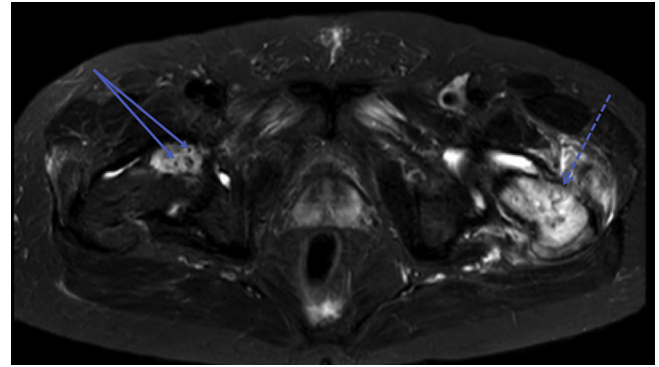


Figure 2 Axial STIR sequence of the pelvis demonstrating two lesions in the proximal femora. The lesion on the right side demonstrates two punctate foci without signal within the lesion (grade 1, solid arrows). The lesion on the left side demonstrates a serpiginous, tubular area without signal, <3 mm in diameter (grade 2, broken arrow).



Figure 3 Sagittal PD sequence demonstrates a lesion in the distal femur. Within the lesion, there are serpiginous, tubular area without signal, <3 mm in diameter (grade 2, broken arrow). In addition, there are multiple serpiginous, tubular areas of signal void, ≥3 mm in diameter (grade 3, solid arrows).

proposed grading system is the first of its kind for the “flow-void” sign to the authors’ knowledge. In the present patient cohort, a statistically significant difference was demonstrated between the type of “flow-void” sign and lesion size. With increasing size of a lesion, the signal voids within the lesion became more conspicuous and more closely resembled vessels. In addition, T2-weighted, PD, and fat-saturated imaging also demonstrated the “flow-void” sign more frequently, with the latter two sequences also demonstrating type 2 and type 3 “flow-void” sign most frequently.

Although this study evaluating the “flow-void” sign in RCC bone metastases constitutes the largest patient cohort

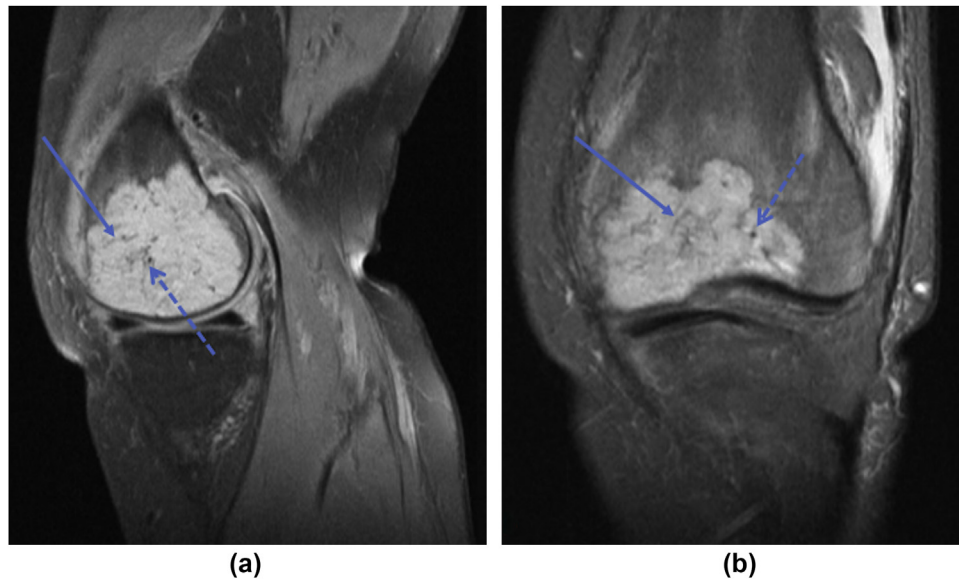


Figure 4 Sagittal fat-saturated PD (a) and coronal STIR (b) images demonstrate a lesion in the distal femur containing both grade 1 (broken arrow) and grade 2 (solid arrow) “flow void” sign.

to the authors’ knowledge, there are limitations to the study. The sensitivity and specificity of the “flow-void” sign was not determined as other bone tumours were not included in the study. In addition, as some patients in this cohort were referred from external institutions with imaging performed elsewhere, there was some heterogeneity across the MRI sequences performed.

In conclusion, the results of the present study indicate that the “flow-void” sign is a common imaging feature within RCC bone metastases. When observed, this sign can be a useful imaging feature in the diagnosis of RCC bone metastases, particularly in cases of occult or previously treated and forgotten RCC.

Conflict of interest

The authors declare no conflict of interest.

References

1. Siegel RL, Miller KD, Jemal A. Cancer statistics, 2017. *CA Cancer J Clin* 2017;**67**(1):7–30.
2. Janzen NK, Kim HL, Figlin RA, et al. Surveillance after radical or partial nephrectomy for localized renal cell carcinoma and management of recurrent disease. *Urol Clin North Am* 2003;**30**(4):843–52.
3. Saitoh H. Distant metastasis of renal adenocarcinoma. *Cancer* 1981;**48**:1487–91.
4. Henriksson C, Haraldsson G, Aldenborg F, et al. Skeletal metastases in 102 patients evaluated before surgery for renal cell carcinoma. *Scand J Urol Nephrol* 1992;**26**:363–6.
5. Althausen P, Althausen A, Jennings LC, et al. Prognostic factors and surgical treatment of osseous metastases secondary to renal cell carcinoma. *Cancer* 1997;**80**:1103–9.
6. Wilner D. Cancer metastasis to bone. In: Wilner D, editor. *Radiology of bone tumors and allied disorders*, vol. 4. Philadelphia, PA: Saunders; 1982. p. 3678–89.
7. Mirra JM. *Bone tumors: clinical, radiologic, and pathologic correlations*. Philadelphia, PA: Lea & Febiger; 1989.
8. Tolia BM, Whitmore Jr WF. Solitary metastasis from renal cell carcinoma. *J Urol* 1975;**114**:836–8.
9. Forbes GS, McLeod RA, Hattery RR. Radiographic manifestations of bone metastases from renal carcinoma. *Am J Roentgenol* 1977;**129**:61–6.
10. Nielsen OS, Munro AJ, Tannock IF. Bone metastases: pathophysiology and management policy. *J Clin Oncol* 1991;**9**:509–24.
11. Tongaonkar HB, Kulkarni JN, Kamat MR. Solitary metastases from renal cell carcinoma: a review. *J Surg Oncol* 1992;**49**:45–8.
12. Choi JA, Lee KH, Jun WS, et al. Osseous metastasis from renal cell carcinoma: “flow-void” sign at MRI. *Radiology* 2003;**228**(3):629–34.
13. Bradley Jr WG. Carmen lecture. Flow phenomena in MRI. *Am J Roentgenol* 1988;**150**:983–94.
14. McKay RR, Kroeger N, Xie W, et al. Impact of bone and liver metastases on patients with renal cell carcinoma treated with targeted therapy. *Eur Urol* 2014;**65**:577–84.
15. Beuselinc B, Oudard S, Rixe O, et al. Negative impact of bone metastases on outcome in clear cell renal cell carcinoma treated with sunitinib. *Ann Oncol* 2011;**22**:794–800.
16. Kollender Y, Bickels J, Price WM, et al. Metastatic renal cell carcinoma of bone: indications and technique of surgical intervention. *J Urol* 2000;**164**:1505–8.
17. Swanson DA, Orován WL, Johnson DE, et al. Osseous metastases secondary to renal cell carcinoma. *Urology* 1981;**18**:556–61.
18. Takashi M, Takagi Y, Sakata T, et al. Surgical treatment of renal cell carcinoma metastases: prognostic significance. *Int Urol Nephrol* 1995;**27**:1–8.
19. Smith EM, Kursh ED, Makley J, et al. Treatment of osseous metastases secondary to renal cell carcinoma. *J Urol* 1992;**148**:784–7.
20. Baloch KG, Grimer RJ, Carter SR, et al. Radical surgery for the solitary bony metastasis from renal-cell carcinoma. *J Bone Jt Surg Br* 2000;**82**:62–7.
21. Durr HR, Maier M, Pfahler M, et al. Surgical treatment of osseous metastases in patients with renal cell carcinoma. *Clin Orthop* 1999;**367**:283–90.
22. Barton PP, Waneck RE, Karnel FJ, et al. Embolization of bone metastases. *J Vasc Interv Radiol* 1996;**7**:81–8.
23. Feltrin LT, Ferreira JR, Mamere AE, et al. Signs of hypervascularization at magnetic resonance imaging in bone metastases from renal cell carcinoma. *Radiol Bras* 2009;**42**:155–7.